Available online at www.sciencedirect.com

ScienceDirect

Mendeleev Commun., 2018, **28**, 178–180

Mendeleev Communications

Electrochemical co-deposition for the synthesis of PtPb electrocatalysts

Yurii M. Maksimov,[a] Boris I. Podlovchenko,*[a] Evgeny A. Vyrko,[a] Stanislav A. Evlashin[b] and Dmitry S. Volkov[a]

[a] *Department of Chemistry, M. V. Lomonosov Moscow State University, 119991 Moscow, Russian Federation. Fax: +7 495 939 0171; e-mail: podlov@elch.chem.msu.ru*

[b] *Skolkovo Institute of Science and Technology, 143026 Moscow, Russian Federation. E-mail: s.evlashin@skoltech.ru*

DOI: 10.1016/j.mencom.2018.03.023

The electrochemical co-deposition of Pt and Pb is a simple one-step method of synthesizing a highly active catalyst for formic acid oxidation reaction.

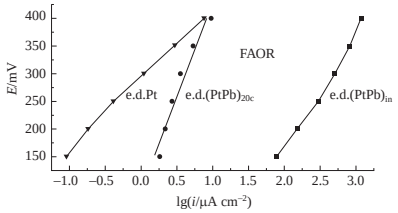

In the context of fuel cells technology, the interest in the synthesis of catalysts highly active in reactions of electrooxidaton of small organic molecules (first of all MeOH and HCOOH) never weakens.[1–5] Pt and Pd are the most active of monocomponent catalysts. However, to date, a large number of studies have shown (*e.g.*, see refs. 3, 4, 6–9) that modification of catalysts of platinum group metals by mixing them with non-noble (or less noble) metals (Ag, Sn, Bi, Pb, *etc.*) often makes it possible to solve simultaneously two problems: to increase the catalyst activity and decrease the consumption of expensive noble metals. In this respect, the mixed Pt–Pb composites synthesized by different methods proved to be promising.[3,6,7,9–13]

Previously, the Pt^0(Pb) composite was obtained by galvanic displacement (GD) of lead from its electrolytic deposit (e.d.Pb) in K_2PtCl_4 solutions.[13] The high catalytic activity of this composite in the electrochemical version of formic acid oxidation reaction (FAOR) was observed. It was interesting to carry out analogous studies for the sample obtained by simultaneous electrodeposition of Pt and Pb from the mixed solution. The advantage of mixed electrodeposits as the model systems for solving fundamental problems of electrocatalysis is that upon their deposition, the nanoparticles are formed in the absence of any precursors of surface-active organic substances.

The aim of this study was (i) to synthesize the Pt–Pb nanocomposite by joint electrodeposition and to characterize the deposit by different physicochemical methods, (ii) to modify the initial deposit by cycling the electrode potential, (iii) to determine the activity of Pt_xPb_y composites in methanol oxidation reaction (MOR) and FAOR.

The co-deposition of Pt and Pb on a glassy carbon plate was carried out at E = –0.2 V (hereinafter the potential values E are given with respect to RHE) from the solution of 0.7×10^{-3} M $PbCO_3$, 10^{-3} M K_2PtCl_4 and 0.1 M $HClO_4$ stirred by a magnetic stir bar ($T^0 = 20\pm1$ °C). The charge of 0.95 C was passed through the electrode. When the deposition of each metal proceeds in the diffusion mode in the absence of hydrogen evolution, this charge should theoretically provide the deposition of 0.5 mg Pt + + 0.5 mg Pb. However, the deviations from the expected deposition conditions proved to be substantial (see below). The deposits were washed with deaerated water and supporting electrolyte solution (0.1 M $HClO_4$) and used in electrochemical measurements. A part of deposits obtained immediately after GD [e.d.$(PtPb)_{in}$] were subjected to additional modification by cycling E in interval of 0.05–1.2 V (v = 20 mV s^{-1}). The samples subjected to potential cycling are designated as e.d.$(PtPb)_{nc}$, where n is the number of cycles.

All PtPb samples were characterized by several physicochemical methods (for reagents and devices used, see refs. 4, 13). The electrochemically active surface area (EASA) was determined based on hydrogen adsorption in 0.1 M $HClO_4$ (210 μC cm^{-2}). The electrocatalytic activity of samples was tested with respect to the stationary currents of MOR and FAOR in the 0.5 M MeOH + + 0.1 M $HClO_4$ and 0.5 M HCOOH + 0.1 M $HClO_4$ solutions, respectively (the criterion of stationary current was its variation by less than 2% min^{-1}).

SEM images show that e.d.$(Pt+Pb)_{in}$ contains spherical particles with very rough surface [Figure 1(*a*),(*b*)]. This allows us to assume that these sufficiently coarse particles (~300 nm) are conglomerates of much finer particles. After multifold potential cycling the

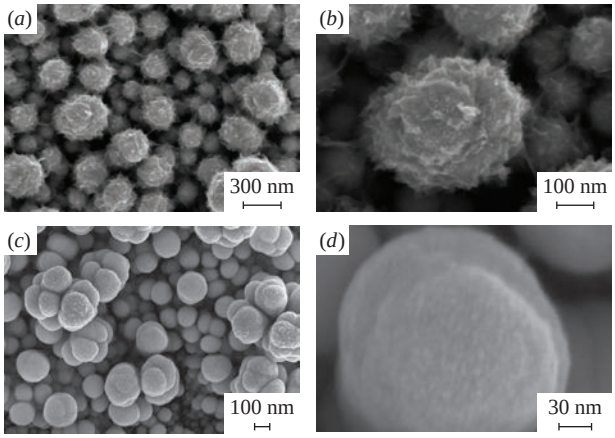

Figure 1 SEM images of (*a*), (*b*) e.d.$(PtPb)_{in}$ and (*c*), (*d*) e.d.$(PtPb)_{20c}$.

Table 1 Bulk and surface composition of e.d.(PtPb) composites.

Sample	Analysis method	Pt (at%)	Pb (at%)
$(PtPb)_{in}$	AES-ISP	51 (157 μg)	49 (160 μg)
	EDX	69	31
	XPS[a]	24 ± 5	76 ± 5
$(PtPb)_{20c}$	EDX	72	28
	XPS	97.4	2.6

[a] Average value based on three measurements.

particles remained spherical. However, their diameter decreased and the surface became sufficiently smooth [Figure 1(*c*),(*d*)].

According to the AES-ICP analysis (Table 1), only ~1/3 of the negative charge passed is consumed in the deposition of Pt and Pb and ~2/3 is used in hydrogen evolution. The results of AES-ICP and EDX (see Table 1) somewhat differ with regard to the volume composition of $(PtPb)_{in}$. Note that the confidence interval of values determined by AES-ICP was ±10% and the scatter of data of EDX analysis in different points of the support surface was also about 10%. On the whole, the results on the bulk composition of $(PtPb)_{in}$ show the presence of deviations, albeit small, from the diffusion mode of metal deposition. After 20-fold potential cycling on the initial sample, its volume composition remained virtually unchanged. This indicates that only relatively weak overall dissolution of Pb and Pt from their alloy occurs during the cycling. Note that, when averaging the EDX results for $(PtPb)_{20c}$, we excluded the point on the surface, for which the content of Pt was found to be close to 100%. This allows us to assume that, at potential cycling up to 1.1 V, at least, Pt and Pb do dissolve according to the anodic scan of CVA,[13] whereas in the cathodic scan, a certain amount of Pt is deposited to form monocomponent particles. The surface of the sample $(PtPb)_{in}$ was ~5 cm^2 (~10 m^2 g^{-1}) and after cycling the total surface decreased by no more than ~10% (Figure 2).

The survey XPS spectra for e.d.$(PtPb)_{in}$ and e.d.$(PtPb)_{20c}$ are qualitatively close, only the peak heights are different. Based on XPS spectra, the surface composition of e.d.$(PtPb)_{in}$ and e.d.$(PtPb)_{20c}$ was assessed (see Table 1). The lead content in the surface layer of e.d.$(PtPb)_{in}$ (thickness 3–4 nm) turned out to be much higher than in the deposit bulk. The reason for this can be the non-uniform deposition of Pt and Pb throughout the depth of PtPb particles and/or additional deposition of lead in the surface layer after the polarization was switched off. The latter may be associated with the important role of lead adatoms (Pb_{ad}) in the formation of upper layers of the deposit at $E > 0$ under open-circuit conditions.[13] During the co-deposition of Pt and Pb at $E < 0$, the adsorption of Pb on Pt may be substantially inhibited by the hydrogen adsorption and evolution. A considerable difference between the bulk and surface compositions was also observed for $(PtPd)_{in}$ deposits synthesized by electrochemical co-deposition.[14]

Cycling of the $(PtPb)_{in}$ potential resulted in a strong depletion of the lead content in the surface layer (down to 2.6 at%, see Table 1). Such a low value for e.d.$(PtPb)_{20c}$ makes it possible to assume the formation of a sufficiently dense Pt shell (the dense Pt shell on Cu contained < 2 at% Cu[15]). This is confirmed by small variations in the bulk composition during potential cycling. Based on the XPS data it was also found that the energy of Pt $4f_{7/2}$ electrons in e.d.(PtPb) is 71.0 eV, which is somewhat lower than for bulk Pt (71.2 eV).[16] Hence, we can assume that intermetallic compounds do not form in considerable amounts in the surface layer of the PtPb alloy. For the preferential deposition of Pt_xPb_y intermetallides,[17] one should expect the stronger decrease in the binding energy of Pt $4f_{7/2}$ electrons.[18]

The CVA curves were obtained for e.d.(PtPb) in the *E* interval of 0.05–1.1 V from the 1st to the 20th cycle without intermediate washing of the electrode with supporting electrolyte solution (see Figure 2). The relatively small changes of the CVA curves adequately agree with the data on the deposit composition (see Table 1). The higher current in the anodic scan at $E > 0.7$ V in the first cycle as compared with the 5th cycle apparently involves, along with the current of oxygen adsorption, the current of lead dissolution from the surface layer, as evidenced by the XPS data (see Table 1). Thus, the electrochemical co-deposit PtPb demonstrates the unexpectedly high stability also at $E > 0.4$ V, although according to estimates,[12,13] both alloys and intermetallides Pt–Pb are thermodynamically unstable at $E > 0.3$ V. It is difficult to unambiguously explain such a behavior of e.d.(PtPb). Presumably, this fact is largely associated with the high potentials of complete removal of Pb_{ad}[13] and/or formation of co-deposits $PtPbO_x$ (according to the Pourbaix diagram, lead oxide should not form at pH ~ 1.0). The presence of lead oxides on the surface of e.d.(PtPb) was demonstrated by XPS spectra of Pb 4*f* electrons.

According to Figure 3, the specific stationary activity of e.d.$(PtPb)_{in}$ in MOR (curve *1*) does not differ strongly from the activity of e.d.Pt (curve *3*) and the effect of Pb is manifested mainly in the increase in the polarization curve slope d*E*/dlg*i*, which points to the larger contribution of dehydrogenation current into the overall current of MOR on e.d.$(PtPb)_{in}$ as compared with e.d.Pt. After cycling the electrode potential, the stationary MOR current on the e.d.$(PtPb)_{20c}$ composite increased to exceed that on e.d.Pt by a factor of ~4 (Figure 3, curve *2*). However, it cannot be ruled out that this effect may be associated to a certain extent with the change in the composition of the final products of MOR (the higher yield of CO_2). In addition, the substantial stationary currents of MOR were observed only at $E \geq 0.5$ V, *i.e.*, in the region of little interest for direct methanol fuel cells.

The much higher activity of Pt with Pb additions is also observed for FAOR (Figure 4), which as a whole adequately agrees with the literature data.[3,6,7,9,12,13] The specific stationary currents of FAOR on e.d.(PtPb) (curve *1* and *2*) exceed such currents on e.d.Pt (curve *3*): at 150 mV, almost by three orders of magnitude for e.d.$(PtPb)_{in}$ and by a factor of 20 for e.d.$(PtPb)_{20c}$; at 300 mV, by a factor of ~400 and 4, respectively. The behavior of e.d.Pb in FAOR qualitatively resembles that of Pt^0(Pb) com-

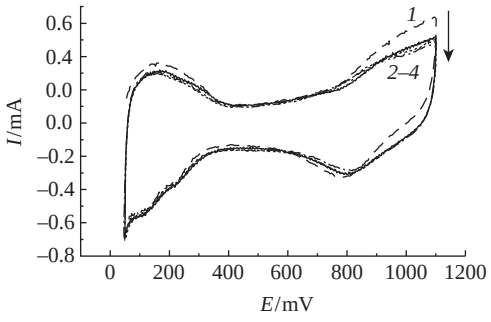

Figure 2 CVA in 0.1 M $HClO_4$ for e.d.(PtPb): (*1*) $(PtPb)_{1c}$, (*2*) $(PtPb)_{5c}$, (*3*) $(PtPb)_{10c}$, and (*4*) $(PtPb)_{20c}$. $v = 20$ mV s^{-1}.

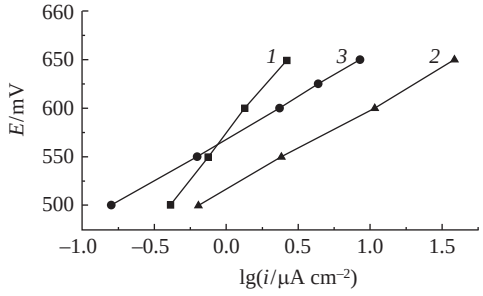

Figure 3 Stationary polarization curves in 0.5 M MeOH and 0.1 M $HClO_4$ solution on electrodes: (*1*) e.d.$(PtPb)_{in}$, (*2*) e.d.$(PtPb)_{20c}$, and (*3*) e.d.Pt (support, GC).

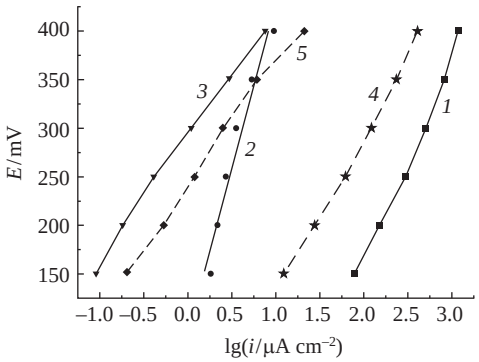

Figure 4 Stationary polarization curves in 0.5 M HCOOH and 0.1 M $HClO_4$ solutions on electrodes: (*1*) e.d.$(PtPb)_{in}$, (*2*) e.d.$(PtPb)_{20c}$, (*3*) e.d.Pt, (*4*) $Pt^0(Pb)_{in}$,[13] and (*5*) $Pt^0(Pb)_{20c}$ (support, GC).[13]

posites prepared by galvanic displacement (curves *4* and *5*[13]): the very high activity of freshly obtained composites and the strong decrease in their activity after potential cycling. However, the quantitative difference is substantial: for the *E* interval of 150–300 mV, which is of the key interest, the specific stationary currents in FAOR on e.d.$(PtPb)_{in}$ and e.d.$(PtPb)_{20c}$ considerably exceed those on Pt^0(Pb)in and $Pt^0(Pb)_{20c}$, respectively (Figure 4, curves *1* and *4*, *2* and *5*). We failed to observe any sufficiently pronounced correlation between the surface composition (according to XPS data) and the activity of samples. The slopes of polarization curves differed strongly from one sample to another. Everything aforesaid points to the complex nature of the promotion effect of lead on the electrocatalytic activity of Pt in FAOR.

According to published data on Pt–Pb composites (including our study[13]), the high activity of e.d.PtPd in FAOR can be associated with the blocking of sites for strongly chemisorbed species which represent a 'poison' for the direct path,[1,2,19] the formation of new active centres, and the changes in the electronic structure of Pt ('electronic effect'). It is difficult to separate the contribution of any of these factors, but it is evident that the effect is determined to a large extent by the length of the Pt/Pb interface and the nature of the contact between atoms and/or clusters of these two metals.[19–21]

Thus, the results of this study show that the electrochemical co-deposition of Pt and Pb from mixed solutions of their salts is a simple one-step method for synthesizing highly active catalysts for FAOR.

This work was supported by the Russian Foundation for Basic Research (project nos. 15-03-03436A and 17-08-01414A) and in part by M. V. Lomonosov Moscow State University Program of Development.

References

1 T. Iwasita, *Electrochim. Acta*, 2002, **47**, 3663.
2 M. Neurock, M. Janik and A. Wieckowski, *Faraday Disscuss.*, 2008, **140**, 363.
3 K. Jiang, H.-X. Zhang, S. Zou and W.-B. Cai, *Phys. Chem. Chem. Phys.*, 2014, **16**, 20360.
4 Yu. M. Maksimov, B. I. Podlovchenko, E. M. Gallyamov, S. A. Dagesyan, V. V. Sen and S. A. Evlashin, *Mendeleev Commun.*, 2017, **27**, 382.
5 A. B. Kuriganova, I. N. Leontyev, A. S. Alexandrin, O. A. Maslova, A. I. Rakhmatullin and N. V. Smirnova, *Mendeleev Commun.*, 2017, **27**, 67.
6 X. H. Xia and T. Iwasita, *J. Electrochem. Soc.*, 1993, **140**, 2559.
7 E. Casado-Rivera, D. J. Volpe, L. Alden, C. Lind, C. Downie, T. Vázquez-Alvarez, A. C. D. Angelo, F. J. DiSalvo and H. D. Abruña, *J. Am. Chem. Soc.*, 2004, **126**, 4043.
8 B. I. Podlovchenko, Yu. M. Maksimov, S. A. Evlashin, T. D. Gladysheva, K. I. Maslakov and V. A. Krivchenko, *J. Electroanal. Chem.*, 2015, **743**, 93.
9 S. Papadimitriou, A. Tegou, E. Pavlidou, G. Kokkinidis and S. Sotiropoulos, *Electrochim. Acta*, 2007, **52**, 6254.
10 M. Bełtowska-Brzezinska, T. Łuczak, J. Stelmach and R. Holze, *J. Power Sources*, 2014, **251**, 30.
11 G. Saravanan, K. Nanba, G. Kobayashi and F. Matsumoto, *Electrochim. Acta*, 2013, **99**, 15.
12 C. Roychowdhury, F. Matsumoto, V. B. Zeldovich, S. C. Warren, P. F. Mutolo, M. J. Ballesteros, U. Wiesner, H. D. Abruña and F. J. DiSalvo, *Chem. Mater.*, 2006, **18**, 3365.
13 B. I. Podlovchenko and Yu. M. Maksimov, *J. Electroanal. Chem.*, 2017, **801**, 319.
14 T. D. Gladysheva, B. I. Podlovchenko, D. S. Volkov and A. Yu. Filatov, *Mendeleev Commun.*, 2016, **26**, 298.
15 B. I. Podlovchenko, T. D. Gladysheva, A. Yu. Filatov and L. V. Yashina, *Russ. J. Electrochem.*, 2010, **46**, 1189 (*Elektrokhimiya*, 2010, **46**, 1242).
16 J. F. Moulder, W. F. Stickle, P. E. Sobol and K. D. Bomben, *Handbook of X-ray Photoelectron Spectroscopy*, eds. J. Chastain and R. C. King, Jr., ULVAC-PHI, Inc., Chigasaki, 1995.
17 *ASM Handbook. Vol. 3. Alloy Phase Diagrams*, eds. H. Okamoto, M. E. Schlesinger and E. M. Mueller, ASM International, Materials Park, OH, 2016.
18 S. Habouti, A. Lahmar, M. Dietze, C.-H. Solterbeck, V. Zaporojtchenko and M. Es-Souni, *Acta Mater.*, 2009, **57**, 2328.
19 B. I. Podlovchenko, Yu. M. Maksimov and K. I. Maslakov, *Electrochim. Acta*, 2014, **130**, 351.
20 B. I. Podlovchenko, Yu. M. Maksimov, K. I. Maslakov, D. S. Volkov and S. A. Evlashin, *J. Electroanal. Chem.*, 2017, **788**, 217.
21 R. S. Batalov, V. V. Kusnetsov, B. I. Podlovchenko and V. A. Zaytsev, *Mendeleev Commun.*, 2017, **27**, 583.

Received: 29th August 2017; Com. 17/5342